

8-psec pulses.

The latter result is consistent with the fact that the momentum randomization time in germanium, at the huge carrier densities achieved here, may be as short as 10^{-14} sec. We can now explain the different widths of the two observed structures. For a band-filling grating effect the response function $A(t)$ is essentially constant over the pulse width and the change in transmitted energy is a measure of the *coherence* of the pulses. Conversely, as the state-filling relaxation time is short compared to the coherence time of the optical pulses then the associated $A(t)$ is essentially a delta function and the transmitted (diffracted) energies measure the *intensity correlation*. We have performed independent measurements that verify the coherence and autocorrelation times to be approximately 2 and 10 psec, respectively, almost precisely the widths of the two features.

In conclusion we have demonstrated that aniso-

tropic state filling in germanium can be achieved at excitation intensities in excess of 1 GW/cm^2 . We have also established that the lifetime associated with the maintenance of anisotropic state filling is less than (and probably considerably less than) a few picoseconds.

This work was supported by the U. S. Office of Naval Research, the Robert A. Welch Foundation, and the North Texas State Faculty Research Fund.

¹C. J. Kennedy, J. C. Matter, A. L. Smirl, H. Weichel, F. A. Hopf, and S. V. Pappu, Phys. Rev. 32, 419 (1974).

²C. V. Shank and D. H. Auston, Phys. Rev. Lett. 34, 479 (1975).

³J. R. Lindle, S. C. Moss, and A. L. Smirl, Phys. Rev. B 20, 2401 (1979).

⁴A. L. Smirl, A. Miller, G. P. Perryman, and T. F. Boggess, J. Phys. (Paris), Colloq. C7, 463 (1981).

⁵D. K. Ferry, Phys. Rev. B 18, 7033 (1978).

Surface Plasmon Coupling in Clusters of Small Spheres

P. E. Batson

IBM Thomas J. Watson Research Center, Yorktown Heights, New York 10598

(Received 19 July 1982)

An inelastic scattering process is observed between 2.5 and 4.0 eV when clusters of 10- to 50-nm-diam aluminum spheres are excited by a 1-nm-diam probe of 100-keV electrons. This inelastic scattering is a maximum when the incident electron probe is positioned within 10 nm of the smaller of two touching spheres. The observed energy and the spatial variation of the scattering probability are consistent with a calculation for a two-sphere system immersed in aluminum oxide.

PACS numbers: 71.45.Gm, 79.20.Kz

Recent theoretical work on light-emitting tunnel junctions formed by small metal particles on metal surfaces,^{1,2} and on the interaction of electromagnetic resonances in surface-enhanced Raman scattering,³ have assumed a model in which the surface plasmon energy is shifted downwards from its normal value by the strong electrostatic interaction between two adjacent small spheres. I report here the first direct observation of such coupling. Briefly, inelastic scattering of fast electrons in clusters of 10- to 50-nm-diam oxide-coated Al spheres shows anomalous peaks in the region 2–5 eV. I identify these excitations as surface plasmons with bispherical symmetry residing within systems of two touching spheres. Both the energy and the spatial

variation of the inelastic scattering are found to agree with calculations similar to those in the above theoretical work.

The Al spheres were formed by evaporation in an atmosphere of Ar at 4 Torr pressure⁴ and collected on a thin carbon substrate which was cooled to liquid-nitrogen temperatures to reduce migration and clustering during the evaporation. The sample was then transferred to a scanning transmission electron microscope⁵ for the inelastic-scattering experiments. This apparatus produces a 1-nm-diam probe of 100-keV electrons which may be positioned with an accuracy of 0.5 nm to allow the selective probing of small regions of single spheres. Electron energy-loss spectra are obtained with a 1-eV energy resolu-

tion and $\sim 1\text{-\AA}^{-1}$ transverse momentum resolution. High magnification images were used to establish the sphere sizes, the oxide thickness, and the relative separation of two adjacent spheres. The inelastic scattering was then obtained for a detailed comparison with the model calculations based on the observed geometry.

The spheres consist of metallic, often single-crystal, Al cores surrounded by ~ 3.6 nm of Al_2O_3 . In this experiment clusters of spheres extend beyond the edge of a crack in the carbon support film, eliminating any substrate scattering. The smallest touching spheres showed oxide contact layers which were about 3.5 nm thick. Touching spheres in the 15-to-25-nm range had an average 1.5-nm oxide contact layer. Larger spheres usually showed no oxide layer between touching spheres. This behavior is consistent with the formation of the oxide layer on exposure to the atmosphere after the evaporation.

Figure 1 compares the electron energy-loss spectra obtained from two different 36-nm-diam spheres. Bulk plasmon losses at 15 eV and spherically symmetric surface plasmon losses near 6.7 eV are prominent in most spheres. Bulk plasmon losses are even present in spheres with Al core diameters as small as 5 nm.⁶ The loss peak at 3.2 eV occurs only when the fast electron passes close to the 36-nm sphere that lies in contact with another, larger sphere. The isolated sphere lay on the carbon support film well away from other spheres. By selectively sampling different regions of the 36-nm sphere and its large neighbor, it was established that the 3.2-eV energy-loss peak occurred only when the probe passed within ~ 10 nm of the 36-nm

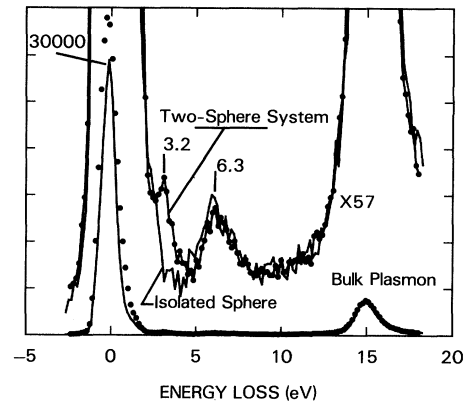


FIG. 1. Inelastic-scattering intensity for two 36-nm, oxide-coated spheres. One, which is in contact with a larger sphere, shows an anomalous peak at 3.2 eV. The isolated sphere shows only the normal surface and bulk loss peaks.

sphere. The 6.7-eV surface peak occurred in the isolated 36-nm sphere and on or near the larger sphere of the two-sphere system. It would appear likely therefore, that the 3.2-eV loss occurs as a result of coupling of fields between the two adjacent spheres, while the 6.7-eV loss is the normal spherically symmetric surface loss occurring on the large sphere.

I have calculated the resonant energies for the dielectric system consisting of two metal spheres with diameters r_1 , r_2 and dielectric constants $\epsilon_1(\omega)$, $\epsilon_2(\omega)$ separated by a small distance d and immersed in a uniform medium with a dielectric constant $\epsilon_0(\omega)$. This system may be treated in bispherical coordinates⁷ where Laplace's equation separates to give solutions, ψ , for the electric potential,

$$\psi \propto F \sum_{n=0}^{\infty} \{A_n \exp[-(n + \frac{1}{2})\mu] + B_n \exp[(n + \frac{1}{2})\mu]\} P_n(\cos \eta), \quad (1)$$

where $F = (\cosh \mu - \cos \eta)^{1/2}$, μ and η are coordinates defined in Fig. 2, and P_n is the Legendre polynomial. I have here assumed azimuthal symmetry about the z axis for simplicity, as shown in the figure. When boundary conditions for ψ and for the electric displacement D are applied at μ_1 and μ_2 , we find a coupled, infinite set of equations for the coefficients A_n and B_n . This set has solutions for frequencies defined by the secular equation

$$\chi^1(\omega)\chi^2(\omega) = \exp[(2n+1)(\mu_1 - \mu_2)], \quad \text{with } \chi^i(\omega) = [\epsilon_0(\omega) - \epsilon_i(\omega)] / [\epsilon_0(\omega) + \epsilon_i(\omega)]. \quad (2)$$

This is a general result for sphere-sphere and sphere-plane systems. For instance, it reproduces the result of Rendell *et al.* [Eq. (11) in Ref. 2] when $\epsilon_1 = -\infty$ and $\mu_2 = 0$. For the present case of two Al spheres with dielectric constant $\epsilon_m(\omega)$, Eq. (2) becomes

$$\epsilon_m(\omega_{\pm}) = -\epsilon_0(\omega_{\pm}) \left\{ \frac{\tanh}{\coth} \right\} \frac{1}{2} (n + \frac{1}{2}) (\mu_1 - \mu_2), \quad (3)$$

where $\epsilon_0(\omega)$ is the frequency-dependent dielectric constant for Al_2O_3 .⁸ Finally, the A_n and B_n are

found, giving well-defined modes ψ_n

$$\begin{aligned} \psi_n(\mu > \mu_1) &\propto F(1 \pm \chi^m) \exp[-(n + \frac{1}{2})(\mu - \mu_1)] P_n(\cos \eta), \\ \psi_n(\mu_2 < \mu < \mu_1) &\propto F \exp[(n + \frac{1}{2})(\mu_1 - \mu_2)/2] \begin{cases} \cosh \\ -\sinh \end{cases} \left\{ (n + \frac{1}{2}) [\mu - (\mu_1 + \mu_2)]/2 \right\} P_n(\cos \eta), \\ \psi_n(\mu < \mu_2) &\propto F(\chi^m \pm 1) \exp[(n + \frac{1}{2})(\mu - \mu_2)] P_n(\cos \eta). \end{aligned} \quad (4)$$

The plus and minus signs (or the upper and lower forms) refer to high- and low-energy solutions which correspond to symmetric and antisymmetric coupling of the small and large sphere fields. An analogous situation occurs in thin metal films where surface plasmon fields on the top and bottom surfaces couple to produce two solutions.⁹ The minus sign produces a charge distribution for $n=0$ which has strong dipole character and which is similar to that shown in Fig. 2. Figure 3 shows the result of Eq. (3) for the antisymmetric solution, for the frequencies ω as a function $\mu_1 - \mu_2$. The coordinate $\mu_1 - \mu_2$ plays the same role that thickness does in the thin film case. For large values of $\mu_1 - \mu_2$ the coupling is weak and the calculated energy is close to the spherically symmetric surface plasmon energy. The symmetric solutions occur near the bulk plasmon energy ω_p , and are not included in Fig. 3. As is evident in Figs. 1 and 4, we find no evidence for the excitation of this solution. I include the spherically symmetric solutions for single

spheres in Fig. 3 for comparison with the bispherical results. These are calculated for the angular momentum quantum number l , for single spheres with radius r , and for an oxide thickness t .⁹ The results are parametrized for inclusion in the figure by setting $\cosh(\mu_1 - \mu_2) = 1 + t/r$.

I have obtained positions of the energy-loss peaks corresponding to the surface plasmons with spherical and bispherical symmetry for a range of sphere sizes. These are shown in Fig. 3 compared to the results of the calculations. The experimental results for bispherical symmetry agree very well with the $n=0$, antisymmetric, solutions of Eq. (3). The observed spread in measurements is probably due to inaccurate determinations of the intersphere spacing d , since the value $\mu_1 - \mu_2$ is very sensitive to small variations in d . It was difficult to measure d with high accuracy when the spheres

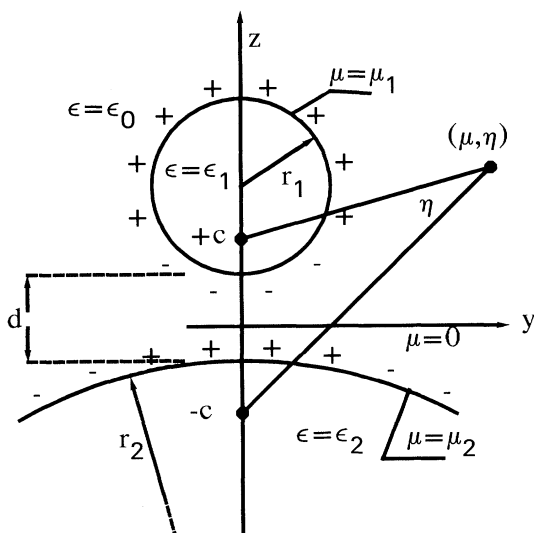


FIG. 2. Two-sphere geometry for the model calculation. The parameter c relates the Cartesian coordinates (x, y, z) to the bispherical coordinates (μ, η) when azimuthal symmetry about z is assumed. r_1 , r_2 , and d uniquely define c , μ_1 , and μ_2 .

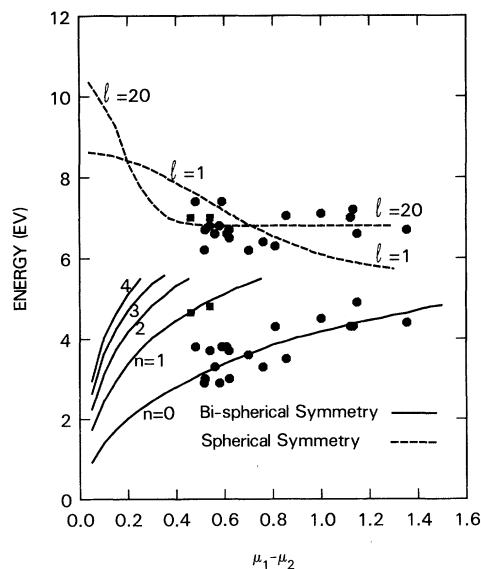


FIG. 3. Comparison of experimental data with the model calculations for spherical and bispherical symmetry. Two experiments with large (> 50 nm) systems show excitation of the $n=1$ mode (squares). The rest of the experiments (circles) were performed on systems smaller than 35 nm.

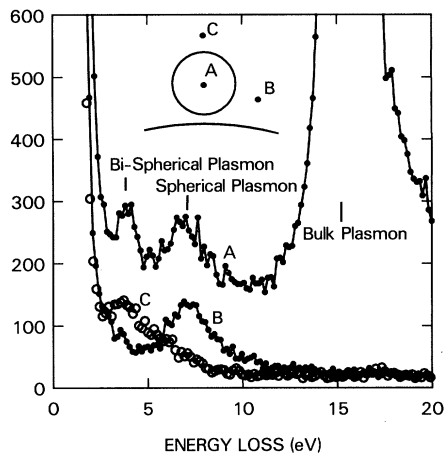


FIG. 4. Comparison of experimental results for three different probe positions near one two-sphere system. The small-sphere radius is about 10 nm. The new mode is not excited when the electron impinges at *B* because the resonance electric field (if excited) would always be perpendicular to the fast electron trajectory.

exceeded about 25 nm in diameter because of the large thickness, in projection, when the system is viewed from a direction which is parallel to the sphere-sphere interface to determine the separation. The experimental results for spherical symmetry appear to be grouped rather loosely about the large-*l* solutions. The results for bispherical symmetry, however, clearly follow the *n*=0 mode. This apparently conflicting behavior will be explained qualitatively below. Some preliminary results, in systems which are greater than 50 nm in size, indicate that bispherical modes with *n*=1 begin to be excited. Figure 3 also shows these results.

The inelastic-scattering probability for fast electrons may be written classically as

$$P_n(\omega, y, z) \propto \int_{-\infty}^{\infty} \vec{x} \cdot \nabla \psi_n(\vec{r}) dx \quad (5)$$

for a fast electron traveling in the +*x* direction. We may evaluate this expression, using Eq. (4), and find for *n*=0 and $\mu_2 \sim -\mu_1$ that the plane $\mu=0$ defines a surface where the *x* component of the electric field is small. Therefore, fast electrons which pass the system within this plane should not lose energy. Figure 4 summarizes the inelastic scattering spectra obtained for three different probe positions to test this possibility. The inelastic loss due to the bispherical mode does not occur in position *B*, close to $\mu=0$, but does occur at position *C*, in spite of the fact that the impact parameter with respect to the center

of the small sphere has remained unchanged. This result, therefore, agrees with the prediction of Eqs. (4) and (5) and strongly supports the assumed model.

I noted above that the scattering favored the small *n* modes in the bispherical case while at the same time it favored the large-*l* modes in the spherical case. Equation (5) reflects the qualitative behavior of $P_n(\omega, y, z)$ when a well-defined ψ_n is known to be present. More often the total response to the passing fast electron will include all modes *n* (or *l* for the spherical case) with relative weightings that will depend strongly on the trajectory of the fast electron. Schmeitz has found in the spherical case that large-*l* modes are excited for small impact parameters, *b*, while small-*l* modes are excited for large *b*.¹⁰ This behavior can be understood by expanding in Legendre polynomials the electric field, due to the fast electron, in a region centered at a distance *b* away from the electron. When *b* is large, the field is roughly uniform and parallel, favoring the small *l* terms. When *b* is small the field is very nonuniform and may even have a finite divergence, thus favoring large-*l* modes. Since the magnitude of this field is largest when *b* is small, we expect most of the excitation to consist of large-*l* contributions.

In the case of the bispherical geometry, the polarizing field must be strong near the interface between the two spheres. We expect, by similar arguments to those above, that large-*n* modes will be excited if the fast electron passes near this interface. However, by the arguments accompanying Fig. 4, inelastic scattering cannot happen in this case because the response field is perpendicular to the electron trajectory there. Scattering can therefore occur only when *b* is large with respect to the interface (e.g., position *C* in the figure) and *n* is constrained to be small.

These results confirm directly that coupling of surface plasmon fields occurs in two-sphere systems. They show, also, that in general, two-sphere and sphere-plane ($\mu_2=0$) systems have simple well-defined eigenmodes. Further, they demonstrate the quantitative variations in the inelastic scattering which occur when small systems are excited in selective positions by very small probes. Work is currently in progress to compare these variations to calculations of inelastic scattering for different electron trajectories.

The author wishes to thank J. Silcox for discussion.

¹D. Hone, B. Mühlischlegel, and D. J. Scalapino, *Appl. Phys. Lett.* **33**, 203 (1978).

²R. W. Rendell, D. J. Scalapino, and B. Mühlischlegel, *Phys. Rev. Lett.* **41**, 1746 (1978).

³For a discussion and extensive references, see P. K. Aravind, A. Nitzon, and H. Metiu, *Surf. Sci.*, **110**, 189 (1981).

⁴S. Yatsuya, S. Kasukabe, and R. Uyeda, *Jpn. J. Appl. Phys.* **12**, 1675 (1973).

⁵This instrument is similar to that described by A. V. Crewe, M. Isaacson, and D. Johnson, *Rev. Sci. Instrum.*

40, 241 (1969).

⁶P. E. Batson, *Solid State Commun.* **34**, 477 (1980).

⁷P. M. Morse and H. Feshbach, *Methods of Theoretical Physics* (McGraw-Hill, New York, 1953), Pt. 2, p. 1298.

⁸C. H. Chen and J. Silcox, *Solid State Commun.* **17**, 213 (1975).

⁹See, e.g., H. Raether, in *Physics of Thin Films*, edited by G. Hass (Academic, New York, 1977), Vol. 9, p. 149.

¹⁰M. Schmeitz, *J. Phys. C* **14**, 1203 (1981).

Fermi Surfaces of Some Dilute Hume-Rothery Alloys

P. T. Coleridge and I. M. Templeton

Division of Physics, National Research Council of Canada, Ottawa, Ontario K1A 0R6, Canada

(Received 15 March 1982)

In dilute alloys, in contrast to pure metals, the measured Fermi-surface volume is too small to accommodate all the electrons. In dilute copper-based heterovalent alloys the discrepancy increases as the solute valence increases but the *anisotropy* of the Fermi-surface changes is found to be approximately rigid-band-like in all alloys. These results are explained quantitatively in terms of the Fermi surface being determined by only those electrons which are scattered coherently.

PACS numbers: 71.25.Hc, 71.55.Dp

In pure metals the Fermi-surface volume is usually considered as being defined by the total number of electrons in the metal. More precisely it is defined as the volume of the constant energy surface corresponding to the chemical potential or Fermi energy in the metal. The equivalence of the two definitions follows from a theorem of Luttinger¹ which was proved for interacting electrons in a periodic potential. Disordered alloys, however dilute, are not periodic and so it is not immediately clear how the Luttinger theorem should be extended to alloys. The concept of the Fermi surface can be extended to alloys by including a self-energy term describing the interaction between conduction electrons and the impurities.² However, there remains the question of how the volume of the Fermi surface is related to the total number of electrons in the alloy. For dilute alloys this is equivalent to considering how the rate of change of Fermi-surface volume, $\Delta V/c$, where c is the concentration of impurities, is related to the valence difference ΔZ , defined as the number of extra conduction electrons per solute atom.

A sensitive and accurate probe of Fermi-surface dimensions is the de Haas-van Alphen (dHvA) effect. In very dilute alloys (of order 0.01 at.%)

the Landau level broadening is sufficiently small that signals can be observed and changes in the dimensions of the Fermi surface (defined as above) can be measured by using high-precision techniques.^{2,3} Although the measurements require a high magnetic field the effect of this on the Fermi-surface dimensions is significant only in the quantum limit.² For the particularly simple case of a rigid-band model the change in cross section ΔA for each extremal orbit is given by

$$c^{-1}\Delta A/A_0 = \frac{2}{3}(m_c/m_{th})\Delta Z, \quad (1)$$

where A_0 is the free-electron cross section, and m_{th} the thermal mass. The anisotropy of the area changes is just proportional to m_c , the cyclotron mass of each orbit. If the small anisotropy of the electron-phonon enhancement is ignored, experimental values can be used for m_c and m_{th} . When experimental results are compared with this simple theory two distinct kinds of breakdown of the model may occur. Firstly, if the Luttinger theorem is invalid the total change of volume of the Fermi surface will no longer be given by $c\Delta Z$. Secondly, the band structure of the alloy may differ from that of the pure metal; then the *anisotropy* of the Fermi-surface changes